ARMY RESEARCH LABORATORY

Analysis of Rigid-Body Effects on Bi-Element Targets

by Nevin L. Rupert
and Fred I. Grace

ARL-TR-1416

July 1997

Army Research Laboratory
Aberdeen Proving Ground, MD 21005-5066

ARL-TR-1416 **July 1997**

Analysis of Rigid-Body Effects on Bi-Element Targets

Nevin L. Rupert, Fred I. Grace
Weapons and Materials Research Directorate, ARL

Abstract

The use of semi-infinite bi-element targets in depth of penetration (DOP) tests initially arose from the need to rank performance of ceramic materials under ballistic impact. However, since ceramics exhibit complex damage responses, interpretation of DOP results for ceramic/metal target combinations can be difficult and sometimes misleading. Thus, recent work utilized bi-element metal/metal targets to determine additional mechanisms present in the earlier DOP ceramic/metal target responses. This demonstrated that significant target interactions are present in either combination in addition to specific damage mechanisms inherent in the ceramic response. The target interactions considered before included shock-induced transient effects at the front target surface and shock wave reflections at the target/target interface. In current work, which considers low-density/low-strength target materials, it has been found that rigid-body penetration is present and needs to be taken into account also. This report investigates rigid-body penetration. The work explores the previously cited mechanisms through experimental work and includes a model to explain results.

Table of Contents

INTENTIONALLY LEFT BLANK.

List of Figures

List of Tables

INTENTIONALLY LEFT BLANK.

1. Introduction

The use of semi-infinite bi-element targets of ceramic/metal in depth of penetration (DOP) testing arose from the need to rank ceramic materials. Performance is measured by the DOP of a long-rod penetrator into a semi-infinite steel back plate after passing through a ceramic applique. The penetrator velocity is held constant while the areal density/thickness of the ceramic is varied over a wide range of values. The DOP vs. applique thickness experiments generate performance maps that provide a means to compare performance of various ceramics in armor designs.

The DOP test method has gained acceptance as a valuable tool for comparative testing and ranking of ceramics. However, previous experimental and analytical work has indicated that such results can be difficult to interpret and sometimes misleading. For example, prior work (Rupert and Grace 1993; Grace and Rupert 1993) has identified a dynamic target interaction effect that can alter perceived performance in a manner similar to the known damage mechanisms that occur in ceramics subject to ballistic impact. The interactions include the shock transient associated with penetrator impact on the target front surface and shock wave reflections at target interfaces. In the previous analysis that considers titanium (Ti), as a surrogate for ceramics, and rolled homogeneous armor (RHA) steel, the shock effects were referred to as a "density effect mechanism" for both metallic and ceramic appliques. The current work considers low-density/lower strength target materials of Ti alloy, as a surrogate for ceramic appliques, and aluminum (Al) second element. The experiments show that rigid-body penetration was present and needed to be taken into account. As with the density effect, the appearance of rigid-body penetration can alter perceived target performance substantially. This report investigates the effects of rigid-body penetration.

2. Materials

2.1 Ti. Since the introduction of Ti and Ti alloys in the early 1950s, these materials have in a relatively short time become the backbone materials for the aerospace, energy, and chemical industries (Bomberger, Froes, and Morton 1985). The combination of a high strength-to-weight ratio, excellent mechanical properties (i.e., strength vs. temperature), and corrosion resistance makes Ti the best material for many critical applications. However, the traditional high cost of Ti alloys has limited their use to applications for which lower cost materials, such as Al and steel, could not be used.

Ti-6A1-4V alloy dominates structural casting applications. This alloy similarly has dominated wrought industry products since its introduction in the early 1950s, becoming the benchmark alloy against which others are compared (Eylon, Nekmlan, and Thorne 1990). With the recent reduction in the cost of Ti alloys, a renewed interest in using Ti as an armor material is taking place. Property data measured from armor plates used in the recent evaluation of low-cost Ti-6A1-4V plates are listed in Table 1.

Table 1. Computational Material Properties

	DU Alloy	Ti 6A1-4V	7039 Al
Density (ρ)	18.6 g/cm^3	4.45 g/cm^3	2.73 g/cm^3
Nominal Strength (S)	1.38 GPa	0.91 GPa	0.45 GPa
Yield Strength (Y_{ys})	NU	0.86 GPa	0.48 GPa[a]
Young's Modulus (E)	NU	113.8 GPa	75 GPa[a]
Plastic Modulus (E_t)	NU	1.9 GPa	0.55 GPa[a]
Sound Velocity	NU	6,070 m/s	5,240 m/s

[a] Zook, Frank, and Silsby 1992.
NU - Not Used

2.2 Al. Interest in Al alloy armor evolved early in World War II from the testing of 2024-T6 and 7075-T6 Al plates (Mascianica 1979). The two alloys showed good fragmentation protection against high-explosive shells and, in some cases, against armor-piercing ammunition. Later, the Al industry cooperated with the Army in developing 7039 Al to military specification MIL-A-46063 (Materials Directorate 1992). This alloy demonstrated improved protection against kinetic energy ammunition. Since then, 7039 Al has become the standard Al armor for the Army. Property data measured from random plates used at the U.S. Army Research

Laboratory (ARL) (formerly the Ballistic Research Laboratory [BRL]) over the past 10 yr are also listed in Table 1.

3. DOP Testing

DOP testing was developed as a means of ranking ceramic materials for ballistic applications (Woolsey, Mariano, and Kokidko 1989; Alme and Bless 1989a, 1989b; Bless, Rosenberger, and Yoon 1987; Woolsey, Mariano, and Kokidko 1990; Frank 1981). Performance is measured by the DOP of a long-rod penetrator into a semi-infinite steel back plate after passing through a ceramic applique. Ceramic performance comparisons are then made between selected baseline materials. We have extended this type of testing to include bi-element metallic targets.

3.1 Projectiles. The projectile used in this study was the 65-g, U-0.75% Ti, long-rod penetrator manufactured by Nuclear Metals, Incorporated. The penetrator had a diameter of 7.70 mm and a length-to-diameter (L/D) ratio of 10. Nominal material properties for these penetrators are as follows: density - 18.6 g/cm^3, hardness - R_c 38-44, yield strength - 800 MPa, ultimate strength - 1,380 MPa, and elongation - 12% (Leonard, Magness, and Kapoor 1992).

3.2 Range Setup. The penetrators were fired from a laboratory gun consisting of a Bofors 40-mm gun breech assembly with a custom-made 40-mm smoothbore barrel. The gun was positioned approximately 3 m in front of the targets. High-speed (flash) radiography was used to record and measure projectile pitch and velocity. Two pairs of orthogonal x-ray tubes were positioned in the vertical and horizontal planes along the shot line (as illustrated in Figure 1). Propellant weight was adjusted for desired nominal velocity of 1,500 m/s. Projectiles with a striking total yaw in excess of 2° were considered a "no test," and those data were disregarded.

3.3 Target Construction. Targets were multihit targets nominally 152.2 mm × 304.4 mm (6 in × 12 in) in size. The first element consisted of a single plate of Ti mechanically clamped to

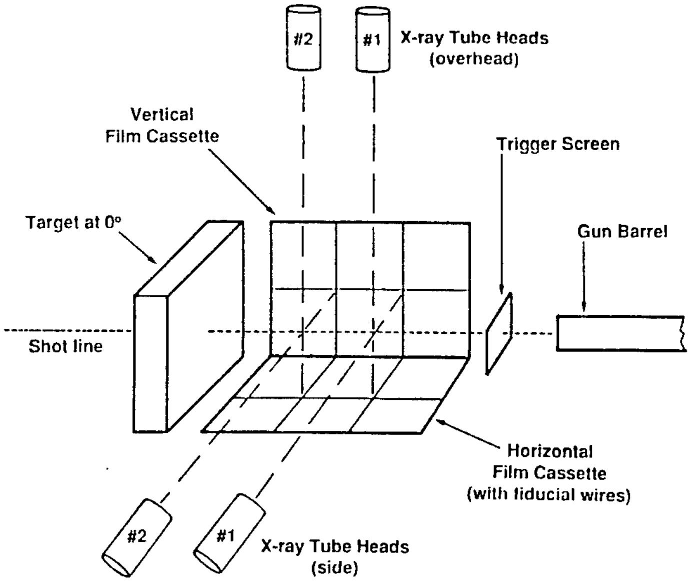

Figure 1. Test Setup.

the second element. Al second elements were constructed from a stack of 76.2-mm (3 in)-thick 7039, MIL-A-46063 Al plates (two to four plates).

4. Test Results

4.1 Baseline Monolithic Ti Data. Monolithic Ti-6A1-4V penetration data for the depleted uranium (DU) penetrator against monolithic Ti-6A1-4V are based on nine tests, where impact velocities ranged from 1,100 m/s to 1,950 m/s (Burkins 1996). Over this range, the data are linear. Thus, an empirical fit to the data was derived in the following form:

$$DOP_{(Ti)} = 0.0949 \left(\frac{mm \cdot s}{m} \right) \cdot V_s - 56.7 \ mm \, , \qquad (1)$$

where V_s is the striking velocity in meters/second, and semi-infinite DOP and the constant are in millimeters. Residual penetrator lengths were not measured during these tests.

4.2 Baseline Monolithic Al Data. Monolithic 7039 Al data for the DU penetrator against Monolithic 7039 Al are limited to 17 tests listed in Appendix A, with impact velocities ranging from 500 m/s to 2,000 m/s (Rupert 1994). Between 1,000 m/s and 2,000 m/s, the data are linear. An empirical fit to the 11 data points was derived as shown:

$$DOP_{(Al)} = 0.1195 \left(\frac{mm \cdot s}{m} \right) V_s - 6.89 \text{ mm}, \tag{2}$$

where V_s is the striking velocity in meters/second, and the semi-infinite DOP and constant are in millimeters. In order to correct for variations in the actual striking velocities, all residual penetration values for metallic bi-element targets were adjusted to a striking velocity of 1,500 m/s by the following correction based on equation (2):

$$DOP_{(Al)} = \text{Measured } DOP_{(Al)} + 0.1195 \left(\frac{mm \cdot s}{m} \right) (1{,}500 \text{ m/s} - V_s). \tag{3}$$

These corrections were made as to minimize the scatter in the bi-element DOP data resulting from round-to-round velocity variations.

4.3 Ti/Al Data. Corrected DOP results for Ti/Al bi-element targets are shown in Figure 2 and listed in Appendix B. (A second-order linear regression curve was fitted to the data using Sigma Plot 5.0 automatic plotting function.) Examination of the regression curve for the ballistic data and the rule of mixtures shows a similar trend as found in the Ti/RHA data (Rupert and Grace 1993).

The rule of mixtures for the study takes the following mathematical form:

$$DOP = DOP_{(2)} \cdot \left[1 - \frac{T_{(a)}}{DOP_{(1)}} \right], \tag{4}$$

where $DOP_{(2)}$ is the semi-infinite DOP value for the second element, $DOP_{(1)}$ is the semi-infinite DOP value for the first element, and $T_{(a)}$ is the applique thickness. Implicit in the rule of mixtures are the following assumptions:

(1) The performance as measured by depth of penetration of the two target elements is linearly additive; there are no interactions or synergistic effects associated with the bi-element target.

(2) The ballistic efficiency of the rear element is constant and independent of the intermediate penetrator length and velocity at the interface between the two elements.

(3) Velocity corrections for the bi-element target are equivalent to velocity corrections for a semi-infinite target of the rear element.

The density effect does not account for the shift of the data up and to the right as in the previous case. However, unlike the RHA/Ti bi-element targets, there are substantial differences in strength, density, and sound velocity of the two metals. Primarily as a result of the aluminum's lower strength and lower density when compared to Ti and RHA, rigid-body penetration within the rear element was introduced to the problem.

5. Modeling

To investigate the performance of Ti/Al targets, two different models were used. One treats target penetration during an initial phase where the rod undergoes erosion, while the other treats target penetration during a subsequent phase where the rod remains rigid. The terms used to differentiate the two processes are "eroding-body" penetration and "rigid-body" penetration, respectively. The quoted qualifiers refer to the state of the penetrator during target penetration.

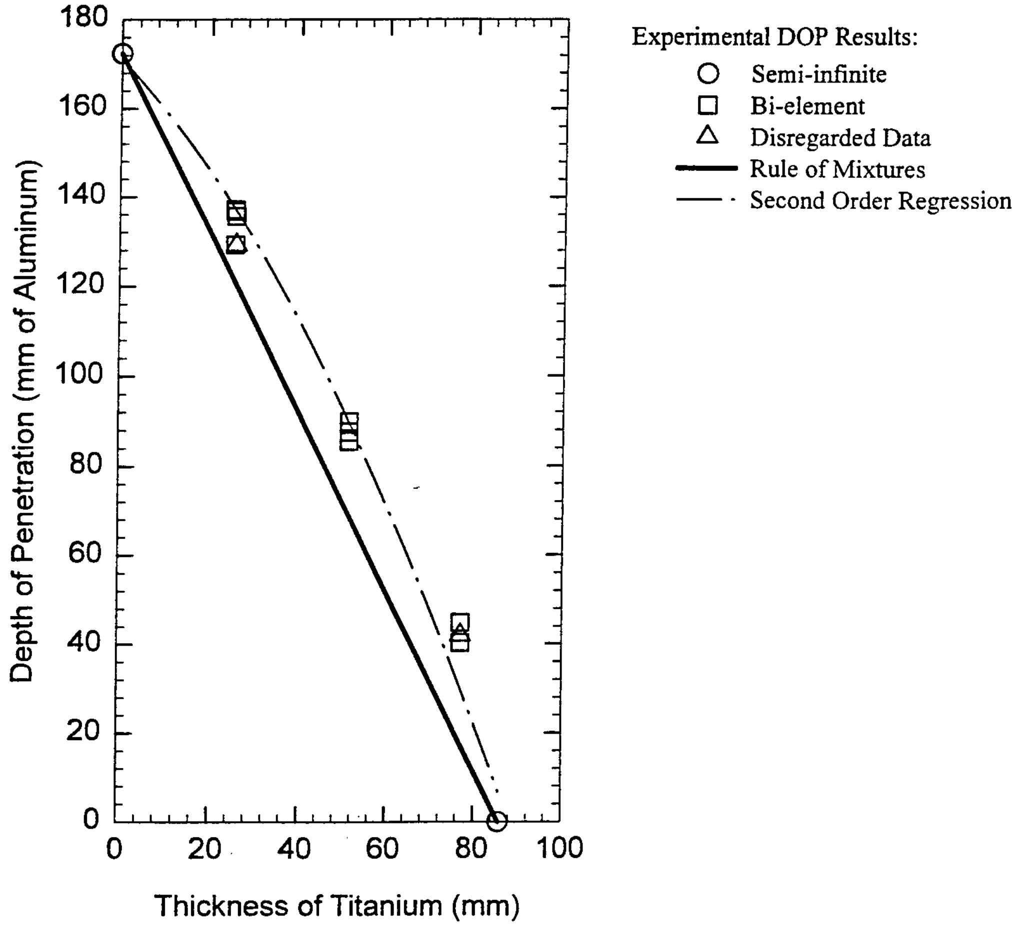

Figure 2. Ti/Al Ballistic Results.

To analyze the dynamic effects that develop and the eroding-body penetration, the nonsteady penetration development of Grace (1993) and its application to bi-element targets by Grace and Rupert (1993) were utilized. There, long-rod penetrators impacting semi-infinite and bi-element targets were considered. For the bi-element targets of interest here, the overall target is semi-infinite and layered as well. The geometry of the bi-element target is shown in Figure 3. Impact conditions are rod impact velocity v_s, initial rod length ℓ_o, and first-element thickness a_o. The backup target, or second element, is semi-infinite metal. Impact conditions for the second layer depend upon rod quantities that exist after penetration through the first layer. These are defined as rod velocity v_1 and rod length ℓ_1. As an extension to previous work (Grace and Rupert 1993), it is assumed that the total penetration P_T in the overall target is the sum of that through each element. This gives

$$P_T = - \int_{\ell_o}^{\ell_1} \left(\frac{u}{v - u} \right)_1 dl - \int_{\ell_1}^{\ell_2} \left(\frac{u}{v - u} \right)_2 dl + P_{RB} \, , \qquad (5)$$

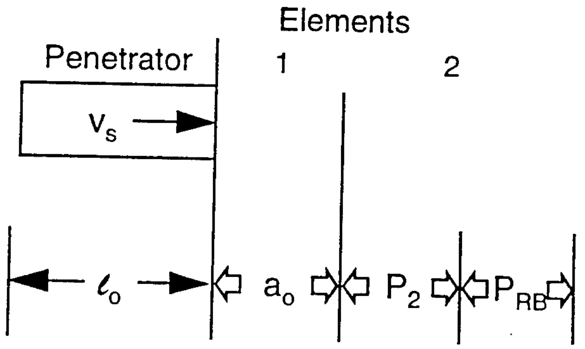

Figure 3. Bi-Element Target Geometry.

where $[u/(v - u)]_1$ and $[u/(v - u)]_2$ are respective penetration velocities divided by the respective penetrator material flow rates for the two elements within the eroding-body phase, and P_{RB} is the subsequent rigid-body penetration within the second element. When the penetrator can overmatch the first element, the first integral on the right-hand side of equation (5) is equal to a_o. However, it is necessary to calculate the penetration through the first element to arrive at penetrator length ℓ_1 and erosion rates $[u/(v - u)]_2$ to be used in the second integral. Also, when rigid-body penetration is involved, the limit ℓ_2 on the second integral will be determined when rod erosion stops. This will result from the condition $(v - u)_2 = 0$, which is given by previous work (Grace 1993), or by a rod-erosion cutoff velocity to be defined subsequently. The DOP or residual penetration P_r into the backup element is given by the second integral plus penetration due to the rigid-body contribution, or

$$P_r = -\int_{\ell_1}^{\ell_2} \left(\frac{u}{v-u}\right)_2 dl + P_{RB} \ . \tag{6}$$

Rod erosion v – u and target erosion u (penetration rate) were given respectively as

$$v - u = (v_s - u_o)\left[1 + \frac{2S_p}{\rho_p (v_s - u_o)^2} \ln\left(\frac{\ell}{\ell_o}\right)\right]^{1/2} \tag{7}$$

and

$$u = u_o \left[1 + \frac{2S_t}{\rho_t u_o^2} \ln\left(\frac{\ell}{\ell_o}\right) \right]^{1/2} . \tag{8}$$

When solving equation (5), penetration into the first element as given by the first integral is calculated stepwise as if the element were semi-infinite. The process continues up to the point where the penetration depth reaches a_o. This provides the starting conditions v_1, u_1, and ℓ_1, for the second integral. Since equations (7) and (8), as written, apply to the first element, their use for the second element requires v_s, u_o, and ℓ_o to be replaced with v_1, u_1, and ℓ_1. The second integral is calculated stepwise up to the point where the rod stops eroding, which provides penetration depth P_2 into the second element during the eroding-body phase, with rod length ℓ_2 and its velocity v_2 as starting conditions for the rigid-body penetration portion of the problem.

Penetration into the first element was calculated using previous methods (Grace and Rupert 1993) that account for the shock transient due to impact at the target front surface and shock wave reflections, due to density and sound velocity changes across the target material interface. Treating the first element as semi-infinite produces a penetration process that ignores possible influences, due to the properties of the backup material. A model was developed to account for the density change across the target material interface and to explore its ability to match the experimental observations (Rupert and Grace 1993). This model uses a simplified version of one-dimensional shock wave propagation to treat the influence on penetration due to shock reflection from a proximate interface. Figure 3 depicts the penetrator/target and bi-element target interfaces of interest. An upper limit for the penetration rate is taken to be the particle velocity u_s associated with the shock wave that is generated by penetrator impact with element 1. Two well-known relations from the theory of shock wave propagation give the pressure p, shock velocity U, and particle velocity u immediately behind the shock and density ρ as where c is a

$$p = \rho\, u\, U, \qquad U = c + gu, \tag{9}$$

velocity of sound, and g is a material constant. Applying these two equations to the penetrator/ target and bi-element target interfaces together with appropriate boundary conditions gives the following expressions used in the current model as

$$u_s = \frac{\rho_p / \rho_l}{1 + \rho_p / \rho_l} v_s, \qquad u_r = (\rho_l / \rho_s) u_i , \tag{10}$$

under simplifications that the sound speeds of the penetrator and targets are taken to be equal, and the variation of shock speed with particle velocity has been ignored. In equation (9), ρ_p is the rod density, u_r is the velocity of material reflected from the interface, and u_i is the incident material velocity. Upon impact, the initial penetration rate at the front surface u_s drops to a quasi-steady value u_o as penetration proceeds to a depth on the order of a penetrator diameter. The model permits the penetration rate to be increased or reduced from u_o. The change has the following form:

$$u_e = u_o + q(u_s - u_o), \tag{11}$$

where u_e is the effective penetration rate, $q\,(u_s - u_o)$ represents an increment of velocity change, and u_o is the rate given by previous theory (Grace 1993, equation [25]). The form of q is arbitrary and is chosen for convenience to include influences generated by the transient and bi-element target interface as

$$q = \pm k \left(\frac{\rho_2}{\rho_1} \right) \left(\frac{\mathrm{DOP}_{(1)} + d - a_o}{\mathrm{DOP}_{(1)}} \right)^2 , \tag{12}$$

where d is rod diameter, and $\mathrm{DOP}_{(1)}$ is the semi-infinite DOP value for the first-element material. The last term on the right-hand side of equation (12) allows the correction to decrease as the reflective wave weakens due to increased distance to the reflective boundary. The ratio of densities appearing in equation (12) takes into account the strength of the reflected wave as indicated by equation (10), and the sign change indicates the direction of material flow. The value for k is chosen so that q does not exceed q = 1 and the penetration rate of equation (11) does not exceed u_s. Equations (5), (7), (8), and (11) give the penetration through the first element and the expected rod length and velocity to be used as starting values in the calculation for DOP as given by equation (6). The final penetrator length ℓ_2 required in the integration of equation (6) is given by the nonsteady penetration theory (Grace 1993).

As indicated, the nonsteady penetration development (Grace 1993) provides the needed parameters at the point where rigid-body penetration begins, but does not account for rigid-body penetration itself. Thus, beyond the penetration contribution given by the second integral, P_2, it is necessary to calculate P_{RB} separately. For present purposes, P_{RB} is determined using the Alekseevshii/Tate penetration algorithm for rigid-body penetration, as presented by Zook, Frank, and Silsby (1992), and takes the following form:

$$P_{RB} = \frac{\rho_p \ell_2}{2 k_t \rho_t} \ln \left[1 + \frac{k_t \rho_t v_2^2}{H} \right] . \qquad (13)$$

The Alekseevshii formulation treats k_t as a shape factor. Tate takes the value for k_t to be 0.5, corresponding to the value that appears in the Bernoulli equation. The target resistance pressure H of 2.21 GPa was calculated from Goodier's expanding spherical cavity analysis (Goodier 1965). Accordingly, the target resistance is as follows:

$$H = \frac{2Y_{ys}}{3} \left[1 + \ln \left(\frac{2E}{3Y_{ys}} \right) \right] + \frac{2\pi^2}{27} E_t , \qquad (14)$$

where Y_{ys} is the target yield strength, E is Young's modulus, and E_t is the slope from the yield point to the ultimate strength point, assuming a bilinear stress-strain behavior curve. Property values used in the modeling are given in Table 1.

In the present calculations, rod erosion was assumed to stop when penetration velocity reached a critical value. That value, u_c, is determined when the pressure on the nose of the penetrator drops below the stress required for rod erosion. The total stress on the rod, due to its flow into the target, is the sum of the dynamic pressure due to its velocity plus the strength of the target, or

$$p_c = \frac{1}{2} \rho_t u_c^2 + S_t \, . \tag{15}$$

Taking values $S_t = 0.625$ GPa for the model's target material dynamic strength and $p_c = 1.38$ GPa for the model's penetrator dynamic strength gives an erosion cutoff velocity of 743 m/s for DU rods into Al targets. Thus, the second integral was solved stepwise until the penetration velocity was reduced to 743 m/s. This gave rod length ℓ_2, velocity v_2, and penetration P_{RB} in the Al at the end of the eroding-body penetration phase.

6. Experimental and Model Results

The current work addresses low-density/lower strength target materials of Ti/Al and the possibility of rigid-body penetration in these targets. The experimental results provided three observations suggesting that at least some rigid-body penetration was taking place in the Al backup targets:

(1) The greater DOPs than expected (based on erosion) in the Al suggested that the penetrator had higher efficiency than it would have had otherwise. This is consistent with rigid-body penetration.

(2) Within the DOP tests, recovered residual penetrators had lengths of 2.0–2.5 rod diameters, whereas 1.0–1.5 factors would be expected under eroding-body penetration only.

(3) Most convincingly, experimental data for penetration of DU rods into semi-infinite aluminum with impact velocities between 500 m/s to 750 m/s exhibited rigid-body penetration, exclusively. Complete uneroded penetrators were recovered from the Al targets.

Figure 4 provides DOP data as a function of Ti applique thickness. The data points on the abscissa and ordinate correspond to semi-infinite targets of penetration by the DU penetrator into Ti (86.4 mm) and Al (172.4 mm), respectively. Penetration calculations were carried out for each of the two cited semi-infinite targets. Results indicated that the semi-infinite Ti was penetrated by eroding-body penetration only because of its higher strength and density as compared to Al. Using nominal strengths for DU and Ti from Table 1 gave a penetration depth into semi-infinite Ti of 85.7 mm. On the other hand, penetration into the Al target resulted from both eroding-body and rigid-body penetration phases. For the Al, the nonsteady theory gave an eroding-body penetration of 138 mm and a rod length of 16.7 mm at the erosion cutoff velocity of 743 m/s. These values and equation (13) provided a calculated rigid-body contribution of 36 mm for a total penetration into Al of 174 mm.

For the bi-element targets, calculations indicated that both eroding-body and rigid-body penetrations were present in the backup Al. Again, 743-m/s erosion cutoff velocity was used. Calculated values for residual penetrator length (rigid-body length) over the range of Ti thicknesses were from 18.7 to 15.2 mm, while the experimentally measured average values varied between 19 and 10 mm. The DOP calculations are presented in Figure 4. The straight solid line connecting the semi-infinite points (Figure 4, curve 3) represent expected results from the rule of mixtures equation (4). The first point to note is that the calculated eroding-body phase (Figure 4, curves 4 and 5) gave DOPs that approach the rule-of-mixture curve for the thicker Ti appliques. The eroding-body calculations are much further beneath the rule of mixture when greater amounts of Al are penetrated in the bi-element target with the thinner Ti sections. The amount of rigid-body penetration is constant and not proportional to the Ti applique thickness as a result of equation (15). While this proposition would presently be difficult to confirm experimentally, the constant cutoff velocity assumed combined with the nearly constant residual

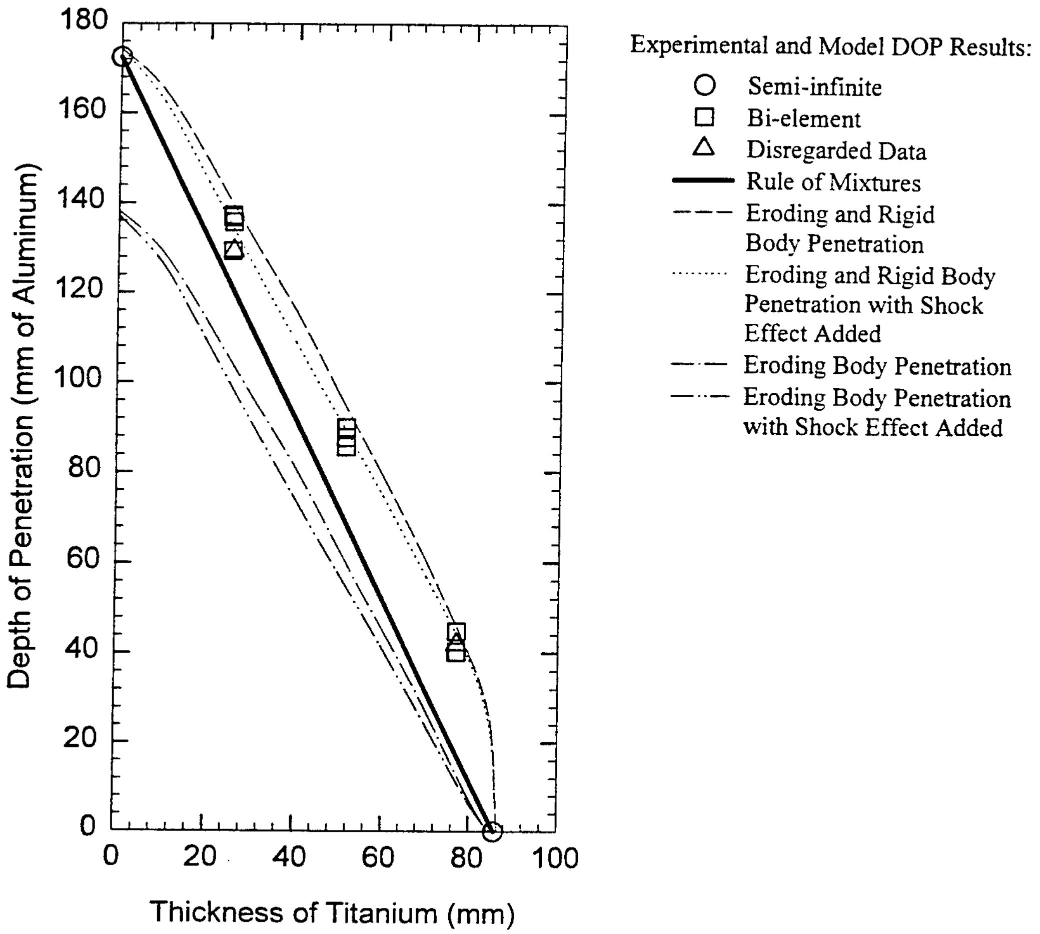

Figure 4. Ti/Al Data and Model Results.

penetrator lengths measured support this proposition as a strong possibility. Additional experimental refinements are being investigated to determine the transition between penetration modes. As expected, there was a slight downward shift of about 6–9% when the shock wave or density effect was taken into account (Rupert and Grace 1993; Grace and Rupert 1993). The upper two curves (Figure 4, curves 1 and 2) represent the total calculated penetration based on eroding-body and rigid-body contributions. Shock effects were not accounted for in the higher curve (Figure 4, curve 1), but were taken into account in the lower one (Figure 4, curve 2). In either case, the rigid-body penetration was about 30% of the total in the backup for thin Ti appliques. It became the major contribution for thick Ti appliques. For the low-strength Al targets considered here, it was necessary to account for rigid-body penetration.

7. Summary and Conclusions

The experiments and penetration analysis provided relative contributions of eroding-body and rigid-body penetration phases. Further, the analysis showed that calculated shock effects in these particular Ti/Al targets influence penetration by about 6–9%. The amount of rigid-body penetration in the backup Al target appears to be nearly constant throughout the range of Ti applique thickness. This accounted for about 30% for thin sections and most of the penetration where the applique was thick. The remainder or initial penetration into the rear element was generated during the rod erosion-based phase. Eroding-body penetration in the backup Al was highest for thin appliques, but contributed little for the thickest ones when the residual rod velocity at the interface approached the cutoff velocity for the aluminum. It is believed that targets having low strength relative to the penetrator will respond in the same fashion, generally. Therefore, the present findings should be applicable to a number of lightweight armor systems, to include composite armor designs.

INTENTIONALLY LEFT BLANK.

8. References

Alme, M., and S. J. Bless. "Experiments to Determine the Ballistic Resistance of Confined Ceramics at Hypervelocity." Draft Report for DARPA, September 1988, published in *Proceedings of the Fifth TACOM Armor Conference*, March 1989a.

Alme, M., and S. J. Bless. "Measuring the Ballistic Resistance of Armor Ceramics." *ATAC Bullet*, 1989b.

Bless, S. J., Z. Rosenberger, and B. Yoon. "Hypervelocity Penetration of Ceramics." *International Journal of Impact Engineering*, vol. 5, pp. 165–171, 1987.

Bomberger, H. B., F. H. Froes, and P. H. Morton. "Titanium-a Historical Perspective." *Titanium Technology: Present Status and Future Trends*, edited by F. H. Froes, D. Eylon, and H. B. Bomberger, pp. 3–17, 1985.

Burkins, M., J. Paige, and J. Hansen. "A Ballistic Evaluation of Ti-6Al-4V vs. Long Rod Penetrators." ARL-TR-1146, U.S. Army Ballistic Research Laboratory, Aberdeen Proving Ground, MD, 1996.

Eylon, D., J. R. Nekmlan, and J. K. Thorne. "Titanium and Titanium Alloy Casting." *Metals Handbook, Properties and Selection: Nonferrous Alloys and Special-Purpose Materials*, 10th ed., vol. 2, pp. 586–591, 1990.

Frank, K. "Armor-Penetration Performance Measures." BRL-MR-03097, U.S. Army Ballistic Research Laboratory, Aberdeen Proving Ground, MD, 1981.

Goodier, J. N. "On the Mechanics of Indentation and in Cratering Solid Targets of Strain-Hardening Metal by Impact of Hard and Soft Spheres." *Proceedings of the Seventh Hyper-Velocity Impact Symposium, Vol. III - Theory*, pp. 215–259, Orlando, FL, 1965.

Grace, F. I., and N. L. Rupert. "Mechanisms for Ceramic/Metal, Semi-Infinite, Bi-Element Target Response to Ballistic Impact," TB-16, *Ballistics '93*, vol. 2, pp. 361–370, 14th International Symposium, Quebec City, Quebec, Canada, 26–29 September 1993.

Grace, F. I. "Non-Steady Penetration of Long Rods Into Semi-Infinite Targets." *International Journal of Impact Engineering*, vol. 14, pp. 303–314, 1993.

Leonard, W. L. Magness, Jr., and D. Kapoor. "Ballistic Evaluation of Thermo-Mechanically Processed Tungsten Heavy Alloys." BRL-TR-3326, U.S. Army Ballistic Research Laboratory, Aberdeen Proving Ground, MD, April 1992.

Mascianica, F. S. "Ballistic Technology of Lightweight Armor 1979." AMMRC-TR-79-1, U.S. Army Materials and Mechanics Research Center, Watertown, MA, February 1979.

Materials Directorate, U.S. Army Research Laboratory. "Armor Plate, Aluminum Alloy, 7039." MIL-A-46063G. Watertown, MA, 30 December 1992.

Rupert, N. L. Unpublished data. U.S. Army Research Laboratory, Aberdeen Proving Ground, MD, 1994.

Rupert, N. L., and F. I. Grace. "Penetration of Long Rods Into Semi-Infinite, Bi-Element Targets," TB-27, *Ballistics '93*, vol. 2, pp. 469–478, 14th International Symposium, Quebec City, Quebec, Canada, 26–29 September 1993.

Woolsey, P., S. Mariano, and D. Kokidko. "Alternative Test Methodology for Ballistic Performance Ranking of Armor Ceramics." *Proceedings of the Fifth TACOM Armor Conference*, March 1989.

Woolsey, P., S. Mariano, and D. Kokidko. "Progress Report on Ballistic Test Methodology for Armor Ceramics." *Proceedings of the First TACOM Combat Vehicle Survivability Symposium*, March 1990.

Zook, J. A., K. Frank, and G. F. Silsby. "Terminal Ballistic Test and Analysis Guidelines for the Penetration Mechanics Branch." BRL-MR-390, U.S. Army Ballistic Research Laboratory, Aberdeen Proving Ground, MD, January 1992.

Appendix A:

Al Data

INTENTIONALLY LEFT BLANK.

Table A-1. Penetration Results for 7039 Al

Striking Velocity (m/s)	Pitch (deg)	Yaw (deg)	DOP (mm)
576	1.00U	0.25L	60.9
741	1.00U	0.25L	125.9
807	1.50U	0.50R	114.4
911	0.50D	0.25R	96.0
1,000	0.50D	0	99.8
1,098	0.25U	0	114.1
1,146	0.50D	0.50L	125.1
1,184	0	0.50L	130.8
1,296	1.25D	1.00R	147.5
1,502	0	0.50R	174.1
1,505	1.00U	0.75R	176.1
1,511	0	0.50R	174.8
1,513	1.00D	1.25R	174.8
1,515	0	1.50R	176.7
1,718	1.75D	0.25L	197.8
2,000[a]	—	—	223.1
2,013	0.25U	0.75L	230.1

[a] Estimated velocity from powder curve.

INTENTIONALLY LEFT BLANK.

Appendix B:

Ti/Al Data

INTENTIONALLY LEFT BLANK.

Table B-1. DOP Results for Ti/Al

Applique Thickness (mm)	Striking Velocity (m/s)	Pitch (deg)	Yaw (deg)	DOP (mm)	Corrected DOP (mm)
25.5	1,354	1.00D	0.75R	111.9	129.3
25.5	1,514	1.50D	0	138.8	137.2
25.7	1,516	1.50D	0.50L	137.6	135.7
25.7	1,522	0.25D	2.25R	139.3	136.7
25.5	1,632	0.50U	0.75R	152.6	136.8
51.5	1,508	0.75D	1.00R	86.5	85.6
51.5	1,511	0.75D	0.75R	89.0	87.7
51.5	1,499	1.00U	0	89.9	89.9
77.0	1,524	0	1.00L	43.2	40.3
77.0	1,524	0	2.50R	44.9	42.0
77.0	1,518	1.75D	1.25R	47.0	44.8

INTENTIONALLY LEFT BLANK.

NO. OF COPIES	ORGANIZATION
2	DEFENSE TECHNICAL INFORMATION CENTER DTIC DDA 8725 JOHN J KINGMAN RD STE 0944 FT BELVOIR VA 22060-6218
1	HQDA DAMO FDQ DENNIS SCHMIDT 400 ARMY PENTAGON WASHINGTON DC 20310-0460
1	CECOM SP & TRRSTRL COMMCTN DIV AMSEL RD ST MC M H SOICHER FT MONMOUTH NJ 07703-5203
1	PRIN DPTY FOR TCHNLGY HQ US ARMY MATCOM AMCDCG T M FISETTE 5001 EISENHOWER AVE ALEXANDRIA VA 22333-0001
1	PRIN DPTY FOR ACQUSTN HQS US ARMY MATCOM AMCDCG A D ADAMS 5001 EISENHOWER AVE ALEXANDRIA VA 22333-0001
1	DPTY CG FOR RDE HQS US ARMY MATCOM AMCRD BG BEAUCHAMP 5001 EISENHOWER AVE ALEXANDRIA VA 22333-0001
1	ASST DPTY CG FOR RDE HQS US ARMY MATCOM AMCRD COL S MANESS 5001 EISENHOWER AVE ALEXANDRIA VA 22333-0001

NO. OF COPIES	ORGANIZATION
1	DPTY ASSIST SCY FOR R&T SARD TT F MILTON THE PENTAGON RM 3E479 WASHINGTON DC 20310-0103
1	DPTY ASSIST SCY FOR R&T SARD TT D CHAIT THE PENTAGON WASHINGTON DC 20310-0103
1	DPTY ASSIST SCY FOR R&T SARD TT K KOMINOS THE PENTAGON WASHINGTON DC 20310-0103
1	DPTY ASSIST SCY FOR R&T SARD TT B REISMAN THE PENTAGON WASHINGTON DC 20310-0103
1	DPTY ASSIST SCY FOR R&T SARD TT T KILLION THE PENTAGON WASHINGTON DC 20310-0103
1	OSD OUSD(A&T)/ODDDR&E(R) J LUPO THE PENTAGON WASHINGTON DC 20301-7100
1	ARL ELECTROMAG GROUP CAMPUS MAIL CODE F0250 A TUCKER UNIVERSITY OF TX AUSTIN TX 78712
1	DUSD SPACE 1E765 J G MCNEFF 3900 DEFENSE PENTAGON WASHINGTON DC 20301-3900
1	USAASA MOAS AI W PARRON 9325 GUNSTON RD STE N319 FT BELVOIR VA 22060-5582

NO. OF COPIES	ORGANIZATION
1	CECOM PM GPS COL S YOUNG FT MONMOUTH NJ 07703
1	GPS JOINT PROG OFC DIR COL J CLAY 2435 VELA WAY STE 1613 LOS ANGELES AFB CA 90245-5500
1	ELECTRONIC SYS DIV DIR CECOM RDEC J NIEMELA FT MONMOUTH NJ 07703
3	DARPA L STOTTS J PENNELLA B KASPAR 3701 N FAIRFAX DR ARLINGTON VA 22203-1714
1	SPCL ASST TO WING CMNDR 50SW/CCX CAPT P H BERNSTEIN 300 O'MALLEY AVE STE 20 FALCON AFB CO 80912-3020
1	USAF SMC/CED DMA/JPO M ISON 2435 VELA WAY STE 1613 LOS ANGELES AFB CA 90245-5500
1	US MILITARY ACADEMY MATH SCI CTR OF EXCELLENCE DEPT OF MATHEMATICAL SCI MDN A MAJ DON ENGEN THAYER HALL WEST POINT NY 10996-1786
1	DIRECTOR US ARMY RESEARCH LAB AMSRL CS AL TP 2800 POWDER MILL RD ADELPHI MD 20783-1145

NO. OF COPIES	ORGANIZATION
1	DIRECTOR US ARMY RESEARCH LAB AMSRL CS AL TA 2800 POWDER MILL RD ADELPHI MD 20783-1145
3	DIRECTOR US ARMY RESEARCH LAB AMSRL CI LL 2800 POWDER MILL RD ADELPHI MD 20783-1145
	ABERDEEN PROVING GROUND
2	DIR USARL AMSRL CI LP (305)

NO. OF COPIES	ORGANIZATION
3	DIR DARPA LTC R KOCHER (3 CPS) 3701 N FAIRFAX DR ARLINGTON VA 22203-1714
3	CDR US ARMY RSCH OFC K LYER K IYER J BAILEY PO BOX 12211 4033 MIAMI BLVD RESEARCH TRIANGLE PARK NC 27709
2	CDR US ARMY MRDEC AMSMI RD ST WF D LOVELACE M SCHEXNAYER REDSTON ARSENAL AL 34898-5250
3	CDR US ARMY TACOM RD&E CENTER AMCPM ABMS SA J ROWE AMSTA RSS J THOMPSON AMSTA RSK S GOODMAN WARRREN MI 48397-5000
1	CDR USA BLVR RD&E CTR STRBE NAN TECH LIBRARY FT BELVOIR VA 22060-5166
6	CDR US ARMY ARDEC SMCAR AAE W J PEARSON TECH LIBRARY PICATINNY ARSENAL NJ 07806-5000
1	PM TANK MAIN ARMNT SYSTEMS SSAE AR TMA MT PICATINNY ARSENAL NJ 07806-5000

NO. OF COPIES	ORGANIZATION
1	PM SURVIVABILITY SYS SFAE ASM SS T T DEAN WARREN MI 48397-5000
1	CDR NGIC W MARLEY 220 SEVENETH AVE CHARLOTTESVILLE VA 22901-5391
1	CDR ERO USARDSG (UK) R REICHENBACH PSC 802 BOX 15 FPO AE 09499-1500
1	USMC MCRDAC PM GRNDS WPNS BR D HAYWOOD FIREPOWER DIV QUANTICO VA 22134
1	CH OF NAVAL RSCH OFC OF NAVAL TECH A J FAULSDITCH ONT 23 BALLSTON TOWERS ARLINGTON VA 22217
1	NAVAL WPNS CTR TECH LIBRARY CHINA LAKE CA 93555
4	CDR NSWC R GARRETT R 12 J FOLTZ R 32 H DEJARNETTE R 32 TECH LIBRARY 10901 NEW HAMPSHIRE AVE SILVER SPRING MD 20903-5000
1	NUSC NEWPORT S DICKINSON CODE 8214 NEWPORT RI 02841
1	NSWC DAHLGREN DIV G 22 ROWE DAHLGREN VA 22448

NO. OF COPIES	ORGANIZATION
1	NAVAL POST GRAD SCHOOL J STERNBERG CODE EW MONTEREY CA 93943
2	MSD ENL W DYESS J FOSTER EGLIN AFB FL 32542-5000
1	BOMBS & WARHEAD BRANCH W COOK MUNITIONS DIVISION EGLIN AFB FL 32542
1	AIR FORCE ARMNT LAB TECH LIBRARY EGLIN AFB FL 32542
1	NEW MEXICO TECH D EMARY TERA GROUP SOCORRO NM 87801
1	AMERICAN EMBASSY BONN DR R ROBINSON UNIT 21701 BOX 165 APO AE 09080
10	DIR SANDIA NATIONAL LABS M KIPP DIV 1533 R GRAHAM DIV 1551 P YARRINGTON D GRADY MS 0821 D CRAWFORD ORG 1533 M FORRESTAL LUK J ASAY MS 0548 R BRANNON MS 0820 M KIPP MS 0820 TECH LIBRARY PO BOX 5800 ALBUQUERQUE NM 87185
1	DEFENSE NUCLEAR AGENCY TECH LIBRARY 6801 TELEGRAPH RD ALEXANDRIA VA 22192
10	DIR LOS ALAMOS NATIONAL LAB G E CORT F663 R KARPP MS 1960 F ADDESSIO F GAC M BURKETT B HOGAN W GASKILL J CHAPYAK MS G787 S MARSH MS 970 M 6 TECH LIBRARY PO BOX 1663 LOS ALAMOS NM 87545
11	DIR LLNL J E REAUGH L 290 M FINGER MS 35 D BAUM D STEINBERG J REAUGH L32 M WILKINS M J MURPHY R GOGOLEWSKI MS L290 R LANDINGHAM L369 R WHIRLEY L122 TECH LIBRARY PO BOX 808 LIVERMORE CA 94550
1	CIA OSWR DSD W WALTMAN ROOM 5P0110 NHB WASHINGTON DC 20505
1	JET PROPULSION LAB M ADAMS IMPACT PHYSICS GROUP 4800 OAK GROVE DR PASADENA CA 91109-8099
4	POULTER LAB D CURRAN R KLOOP L SEAMAN D SHOCKEY SRI INTERNATIONAL 333 RAVENSWWOD AVE MENLO PARK CA 94025

NO. OF COPIES	ORGANIZATION
1	UNIV OF DAYTON R HOFFMAN 300 COLLEGE PARK DAYTON OH 45469
6	INST FOR ADV TECH UNIV OF TX AT AUSTIN H FAIR S BLESS D LITTLEFIELD M NORMANDIA R SUBRANMANIAN T KIEHNE 4030 2 W BRAKER LN AUSTIN TX 78759
3	UNIV OF DAYTON RSRCH INST N BRAR A PIEKUTOWSKI D GROVE KLA14 300 COLLEGE PARK DAYTON OH 45469-0182
2	THE PENN STATE UNIV COLLEGE OF ENGR DR T KRAUTHAMMER DR R QUNEEY UNIV PARK PA 16802
2	SOUTHWEST RSRCH INST C ANDERSON J RIEGEL 6220 CULEBRA RD SOUTHWEST SAN ANTONIO TX 78238
2	UNIV OF CA SAN DIEGO S NEMAT NASSER M MEYERS DEPT OF APPLIED MECHS & ENGR SVCS RO11 LA JOLLA CA 92093-0411
2	CA RSCH & TECH CORP ROBERT BROWN DENNIS ORPHAL 5117 JOHNSON DR PLEASONTON CA 94566

NO. OF COPIES	ORGANIZATION
2	BROWN UNIV M CLIFTON S SUNDARAM DIV OF ENGR PROVIDENCE RI 02912
1	ROCKWELL INTL ROCKETDYNE DIV J MOLDENHAUER 6633 CANOGA AVE HB 23 CANOGA PK CA 91303
2	ALLIED SIGNAL L LIN PO BOX 31 PETERSBURG VA 23804
1	MCDONNELL DOUGLAS HELICOPTER L R BIRD MS 543 D216 5000 E MCDOWELL RD MESA AZ 85205
1	AEROJET PRECISION WPNS DEPT 5131 T W JOSEPH CARLEONE 1100 HOLLYVALE AZUSA CA 91702
1	PHYSICS INTL JIM COFFENBERRY 2700 MERCED ST PO BOX 5010 SAN LEANDRO CA 94577
1	BOEING CORP T M MURRAY MS 84 84 PO BOX 3999 SEATTLE WA 98124
1	NUCLEAR METALS INC R QUINN 2229 MAIN ST CONCORD MA 01742

NO. OF COPIES	ORGANIZATION
3	DYNA EAST CORP P C CHOU R CICCARELLI W FLIS 3201 ARCH ST PHILADELPHIA PA 19104
2	ALLIANT TECHSYSTEMS INC G R JOHNSON C CANDLAND MN 48 2700 7225 NORTHLAND DR BROOKLYN MN 55428
2	GENERAL RSCH CORP ALEX CHARTERS TOM MENNA PO BOX 6770 SANTA BARBARA CA 93160-6770
1	S CUBED R SEDGWICK PO BOX 1620 LA JOLLA CA 92038-1620
2	ORLANDO TECH INC D MATUSKA J OSBORN PO BOX 855 SHALIMAR FL 32579
1	KAMAN SCIENCES CORP D BARNETTE PO BOX 7463 CO SPRINGS CO 80933-7463
1	LIVERMORE SOFTWARE TECH CORP JOHN O HALLQUIST 2876 WAVERLY WAY LIVERMORE CA 94550
2	MARTIN MARIETTA MISSILE SYSTEMS C E HAMMOND MP 004 L WILLIAMS MP 126 PO BOX 555837 ORLANDO FL 32855-5837

NO. OF COPIES	ORGANIZATION
1	BATTELLE DALE TROTT 505 KING AVE COLOUMBUS OH 43201
1	ZERNOW TECH SVCS INC LOUIS ZERNOW 425 W BONITA AVE SUITE 208 SAN DIMAS CA 91773
1	OLIN FLINCHBAUGH DIV RALF CAMPOLI 200 E HIGH ST PO BOX 127 RED LION PA 17356
2	E I DUPONT CO OSWALD BERGMANN BRIAN SCOTT BRANDYWINE BLDG RM 12204 WILMINGTON DE 19898
3	SIMULA INC R HUYETT G GRACE G YANIV 10016 S 51ST ST PHOENIX AZ 85044
1	LANXIDE CORP 1300 MARROWS RD PO BOX 6077 NEWARK DE 19714
1	BRIGGS CO J BACKOFEN 2668 PETERBOROUGH ST HERNDON VA 22071
1	SCHWARZKOPFF TECH CORP E KOSINISKI 35 JEFFREY AVE HOLLISTON MA 01746
1	PRIMEX CORP. D EDMONDS 10101 9TH ST N ST PETERSBURG FL 33716

NO. OF COPIES	ORGANIZATION
1	BATTELLE DR D TROTT 505 KING AVE COLUMBUS OH 43201
1	RAYTHEON CO R LLOYD PO BOX 1201 TEWKSBURY MA 01876
1	COORS CERAMICS CO MR R PARICIO STRUCTURAL DIV 600 NINTH ST GOLDEN CO 80401
1	INGALLS SHIPBUILDING CBI 01 MR P GREGORY PO BOX 149 PASCAGOULA MS 39567
4	UNITED DEFENSE LP V HORVATICH R RAJAGOPAL M MIDDIONE J MARROW PO BOX 359 SANTA CLARA CA 95052-0359
1	ALME AND ASSOC M ALME 9650 SANTIAGE RD STE 102 COLUMBIA MD 21045
3	LANXIDE ARMOR PRODUCTS K LEIGHTON V KELSEY R WOLFE 1300 MARROWS RD NEWARK DE 19714-6077
2	AERONAUTICAL RSRCH ASSOC R CONTILLIANO J WALKER 50 WASHINGTON RD PRINCETON NJ 08540

NO. OF COPIES	ORGANIZATION
1	THE CARBORUNDUM CO R PALIA PO BOX 1054 NIAGRA FALLS NY 19302
3	CERCOM INC R PALICKA A EZIS G NELSON 1960 WATSON WAY VISTA CA 92083
1	CENTURY DYNAMICS INC N BIRNBAUM 7700 EDGEWATER DR SUITE 626 OAKLAND CA 94621
1	APPLIED RSRCH ASSOCS INC J YATTEAU 5941 SO MIDDLEFIELD RD SUITE 100 LITTLETON CO 801123
1	ADELMAN ASSOC C CLINE 3301 EL AMINO RIAL SUITE 280 ATHERTA CA 94027
1	CYPRESS INTERNATIONAL A CAPONECCHI 1201 E ABINGDON DR ALEXANDRIA VA 22314
1	DOW CHEMICAL INC K EPSTEIN ORDNANCE SYS 800 BUILDING MIDLAND MI 48667
1	CALKINS R&D INC N CALKINS 515 SEWARD PK AVE ALBUQUERQUE NM 87123
1	KERAMONT CORPORATION E SAVRUN 4231 S FREEMONT AVE TUSCON AZ 85714

NO. OF COPIES	ORGANIZATION
1	SAIC J FURLONG MS 264 1710 GOODRIDGE DR PO BOX 1303 MCLEAN VA 22102
2	ALLIANT TECHSYSTEMS INC T HOLMQUIST G JOHNSON 7225 NORTHLAND DR BROOKLYN PARK MN 55428
2	GDLS W BURKE J ERIDON PO BOX 2094 WARREN MI 48090
1	BATTELLE EDGEWOOD A RICCHIAZZI 2113 EMMORTON PARK RD EDGEWOOD MD 21040
1	CORNING INC S HAGG SP DV 22 CORNING NY 14831
1	COORS CERAMICS CO STRUCTURAL DIV 600 NINTH ST GOLDEN CO 80401
1	O GARA HESS & EISENHARDT C WILLIAMS 9113 LE SAINT DR FAIRFIELD OH 45014
1	R J EICHELBERGER 409 W CATHERINE ST BEL AIR MD 21014-3613

NO. OF COPIES	ORGANIZATION
	ABERDEEN PROVING GROUND
63	DIR USARL AMSRL-WM-MF, D DANDEKAR S CHOU (16 CPS) AMSRL-WM-TA, W GILLICH T HAVEL W BRUCHEY S BILYK M BURKINS J DEHN G FILBEY W GOOCH D HACKBARTH G HAUVER E HORWATH G BULMASH Y HUANG M KEELE H MEYER E RAPACKI W ROWE J RUNYEON N RUPERT (10 CPS) M ZOLTOSKI M DUFFY AMSRL-WM-TC, W DE ROSSET L MAGNESS W WALTERS F GRACE (6 CPS) E KENNEDY K KIMSEY AMSRL-WM-TD, K FRANK D DIETRICH S SEGLETES T WRIGHT AMSRL-WM-TB, M LAMPSON

NO. OF COPIES	ORGANIZATION
3	FRANHOFER INSTITUT FÜR KURZZEITDYNAMIK ERNST MACH INSTITUT H SENF E STRAßBURGER H ROTENHÄUSLER HAUPTSTRASSE 18 D 79 576 WEIL AM RHEIN GERMANY
3	FRANHOFER INSTITUT FÜR KURZZEITDYNAMIK ERNST MACH INSTITUT THOMA A STILP V HOHLER ECKERSTRAßE 4 D 79 104 FREIBURG GERMANY
3	DEUTSCH FRANZÖSISCHES FORSCHUNGSINSTITUT SAINT LOUIS H ERNST H LERR K HOOG CÉDEX 5 RUE DU GÉNÉRAL CASSAGNOU F 68301 SAINT LOUIS FRANCE
5	DEFENCE RSRCH AGENCY W CARSON T HAWKINS B SHRUBSALL C FREW I CROUCH CHOBHAM LANE CHERTEY SURRETY KT16 OEE UNITED KINGDOM
1	DEFENCE RSRCH AGENCY T BARTON FT HALSTEAD SEVEN OAKS KENT TN14 7BP UNITED KINGDOM
1	BATTELLE INGENIEURTECHNIK GMBH W FUCHE DUESSELDORFLER STR 9 D 65760 ESCHBORN GERMANY
1	DEUTSCHE AEROSPACE AG M HELD POSTFACH 12 40 D 86 523 SCHROBENHAUSEN GERMANY
5	RAPHAEL BALLISTICS CENTER Y PARTOM G ROSENBERG M MAYSELESS Z ROSENBERG Y YESHURUN BOX 2250 HAIFA 31021 ISRAEL
1	DYNAMEC RSRCH AB Å PERSSON PARADISGRÄND 7 S 151 36 SÖDERTÄLJE SWEDEN
1	DEFENCE RESEARCH ESTABLISHMENT SUFFIELD C WEICKERT BOX 4000 MEDICINE HAT ALBERTA TIA 8K6 CANADA
4	CENTRE DE RECHERCHES ET D'ETUDES D'ARCUEIL F TARDIVAL C COTTENNOT S JONNEAUX H ORSINI 16 BIS AVENUE PRIEUR DE LA CÔTE D'OR F 94114 ARCUEIL CÉDEX FRANCE

NO. OF COPIES	ORGANIZATION
1	INGENIEURBÜRO DEISENROTH F DEISENROTH AUF DE HARDT 33 35 D 5204 LOHMAR 1 GERMANY
1	CONDAT K THOMA MAXILLANSTR 28 8069 SCHEYERN FERNHAG GERMANY
1	EMBASSY OF AUSTRALIA DR R L WOODWARD 1601 MASS AVE NW WASHINGTON DC 20036-2273
3	SWEDISH DEFENCE RSRCH ESTABLISHMENT B JANZON I MELLGARD L HOLMBERG BOX 551 S 147 25 TUMBA SWEDEN
2	TNO PRINS MAURITS LAB H PASMAN R YSSELSTEIN PO BOX 45 2280 AA RIJSWIJK LANGE KLEIWEG 137 RUSWIJK NETHERLANDS
2	DEFENCE TECHNOLOGY AND PROCUREMENT AGENCY G LAUBE W ODERMATT BALLISTICS WEAPONS AND COMBAT VEHICLE TEST CENTER CH 3602 THUN SWITZERLAND
1	CELSIUS MATERIAL TEKNIK KARLSKOGA AB L HELLNER S 691 80 KARLSKOGA SWEDEN
1	SWISS FEDERAL ARMAMENT WORKS W LANZ ALLMENDSSTRASSE 86 CH 3602 THUN SWITZERLAND
1	HIGH ENERGY DENSITY RSRCH CENTER G KANEL V FORTOV IZHORSKAYA 13 19 MOSCOW 127412 RUSSIAN REPUBLIC
1	IOFFE PHYSICO TECHNICAL INSTITUTE A KOZHUSHKO ST PERTERBURG 194021 RUSSIAN REPUBLIC
4	AERNAUTICAL & MARITIME RESEARCH LAB N BURMAN S CIMPOERU G WESTON E GELLERT PO BOX 4331 MELBOURNE VIC 3001 AUSTRALIA
1	TECHNION INSTITUTE OF TECHNOLOGY FACULTY OF MECHANICAL ENG. S BODNER TECHNION CITY HAIFA 32000 ISRAEL
2	FEDERAL MINISTRY OF DEFENCE DIRECTORATE FOR EQUIPMENT & TECHLAND RÜ V 2 D HAUG L REPPER POSTFACH 1328 53003 BONN GERMANY
1	CENTER d'ETUDES GRAMAT J CAGNOUX 46500 GRAMAT FRANCE

REPORT DOCUMENTATION PAGE

Form Approved
OMB No. 0704-0188

1. AGENCY USE ONLY *(Leave blank)*

2. REPORT DATE
July 1997

3. REPORT TYPE AND DATES COVERED
Final, October 1993 - February 1994

4. TITLE AND SUBTITLE
Analysis of Rigid-Body Effects on Bi-Element Targets

5. FUNDING NUMBERS
N/A

6. AUTHOR(S)
Nevin L. Rupert and Fred I. Grace

7. PERFORMING ORGANIZATION NAME(S) AND ADDRESS(ES)
U.S. Army Research Laboratory
ATTN: AMSRL-WM-TA
Aberdeen Proving Ground, MD 21005-5066

8. PERFORMING ORGANIZATION REPORT NUMBER
ARL-TR-1416

9. SPONSORING/MONITORING AGENCY NAMES(S) AND ADDRESS(ES)

10. SPONSORING/MONITORING AGENCY REPORT NUMBER

11. SUPPLEMENTARY NOTES
The report was originally given at the 5th Annual TACOM Combat Vehicle Survivability Symposium, 28 Feb - 3 Mar 94, in Monterey, CA, and is published in the proceedings. Later experimental data were added in this report.

12a. DISTRIBUTION/AVAILABILITY STATEMENT
Approved for public release; distribution is unlimited.

12b. DISTRIBUTION CODE

13. ABSTRACT *(Maximum 200 words)*

The use of semi-infinite bi-element targets in depth of penetration (DOP) tests initially arose from the need to rank performance of ceramic materials under ballistic impact. However, since ceramics exhibit complex damage responses, interpretation of DOP results for ceramic/metal target combinations can be difficult and sometimes misleading. Thus, recent work utilized bi-element metal/metal targets to determine additional mechanisms present in the earlier DOP ceramic/metal target responses. This demonstrated that significant target interactions are present in either combination in addition to specific damage mechanisms inherent in the ceramic response. The target interactions considered before included shock-induced transient effects at the front target surface and shock wave reflections at the target/target interface. In current work, which considers low-density/low-strength target materials, it has been found that rigid-body penetration is present and needs to be taken into account also. This report investigates rigid-body penetration. The work explores the previously cited mechanisms through experimental work and includes a model to explain results.

14. SUBJECT TERMS
penetration modeling, Rupert-Grace penetration model, Grace-Tate penetration theory, depth-of-penetration tests, ceramics, rigid-body penetration

15. NUMBER OF PAGES
36

16. PRICE CODE

17. SECURITY CLASSIFICATION OF REPORT
UNCLASSIFIED

18. SECURITY CLASSIFICATION OF THIS PAGE
UNCLASSIFIED

19. SECURITY CLASSIFICATION OF ABSTRACT
UNCLASSIFIED

20. LIMITATION OF ABSTRACT
UL

NSN 7540-01-280-5500

Standard Form 298 (Rev. 2-89)
Prescribed by ANSI Std. 239-18 298-102

INTENTIONALLY LEFT BLANK.

USER EVALUATION SHEET/CHANGE OF ADDRESS

This Laboratory undertakes a continuing effort to improve the quality of the reports it publishes. Your comments/answers to the items/questions below will aid us in our efforts.

1. ARL Report Number/Author ARL-TR-1416 (Rupert) Date of Report July 1997

2. Date Report Received ____

3. Does this report satisfy a need? (Comment on purpose, related project, or other area of interest for which the report will be used.) ____

4. Specifically, how is the report being used? (Information source, design data, procedure, source of ideas, etc.) ____

5. Has the information in this report led to any quantitative savings as far as man-hours or dollars saved, operating costs avoided, or efficiencies achieved, etc? If so, please elaborate. ____

6. General Comments. What do you think should be changed to improve future reports? (Indicate changes to organization, technical content, format, etc.) ____

CURRENT ADDRESS

Organization

Name E-mail Name

Street or P.O. Box No.

City, State, Zip Code

7. If indicating a Change of Address or Address Correction, please provide the Current or Correct address above and the Old or Incorrect address below.

OLD ADDRESS

Organization

Name

Street or P.O. Box No.

City, State, Zip Code

(Remove this sheet, fold as indicated, tape closed, and mail.)

(DO NOT STAPLE)